

TABLE III. Comparison of the clustering characteristics from different models. Energies are in eV.

	Born-Mayer <sup>a</sup>	Morse <sup>b</sup>	Present
$E_{1V}^M$	0.43	0.69	1.32
$E_{2V}^B$	0.06	0.53	0.25
$E_{2V}^M$	0.07	0.03	0.90
$E_{3V}^B$	0.46	2.23	0.76
3V configuration	filled tetrahedron	equilateral triangle	equilateral triangle
$E_{4V}^B$	0.7	3.85	1.51
4V configuration	complex	{111}	tetrahedron
$E_{1I}^M$	0.05	0.15	0.15
$E_{2I}^B$	0.61		1.16
$E_{2I}^M$	0.08		0.29

<sup>a</sup> See Refs. 10–12.<sup>b</sup> See Ref. 7.

to 1.08 eV and in nickel from 1.35 to 1.55 eV. Thus the nickel calculations agree better, but not strikingly so. The copper divacancy binding and migration energies are thought to be about 0.1 and 0.6 eV, respectively, while the nickel divacancy migration energy is in the range of 0.8–1.0 eV. Especially with regard to the divacancy migration energy, the Born-Mayer and Morse

results are in conflict with the data, whereas the present calculations are in agreement. The single-interstitial results were discussed previously,<sup>13</sup> and no reliable interstitial-clustering data are available.

The primary difference between the present calculations and those using either Born-Mayer or Morse interactions is that the interaction used here gives rise to a nearest-neighbor “bond” which must be broken if the atoms are to be separated at all. The Born-Mayer interaction is purely repulsive and the Morse, although it has an attractive tail binding atoms together, is long in range, so that motions of the order of a nearest-neighbor distance do not involve making or breaking the “bond” between atoms. It is the existence of this bond which gives rise to reasonable values of vacancy and divacancy migration energies in the present calculations.

#### ACKNOWLEDGMENTS

It is a pleasure to acknowledge stimulating discussions with Dr. G. J. Dienes, Dr. G. H. Vineyard, and Dr. A. C. Damask during the course of this work.

## Dislocation Velocities in a Two-Dimensional Model\*

W. F. HARTL† AND J. H. WEINER

Department of Mechanical Engineering, Columbia University, New York, New York

(Received 27 December 1965)

The dynamics of an edge dislocation in a two-dimensional crystal model are investigated using a localized unstable normal mode of vibration of the model. The model used is a simple-cubic lattice with linear central and noncentral nearest-neighbor interactions and a piecewise linear restoring force between atoms on the slip plane. The atoms below the slip plane are fixed. Lattice parameters are chosen to allow specific stable and unstable configurations of the lattice, and it is assumed that the dislocation progresses by passing alternately through stable and unstable states. It is found that there is one localized unstable mode of vibration whose components are very large in the neighborhood of the dislocation. This localized mode is used to approximate dislocation motion in the unstable state, and it is altered—by symmetrizing it with respect to the stable lattice configuration—to approximate motion in the stable state. Two coordinates, given by harmonic equations of motion, then characterize the dynamics of the dislocation. The relation between the two coordinates gives an energy-loss mechanism which leads to a steady-state dislocation velocity when a shear stress is applied to the lattice. Transient and steady-state velocities and the minimum stress necessary to maintain a steady-state velocity are calculated. The same quantities are found using computer simulation of a finite lattice, and a comparison is made. Reasonably good agreement is found for velocities up to about 0.7 times the velocity of sound in the continuum in the direction of slip. The analytic theory underestimates the minimum stress necessary to maintain a steady-state velocity.

### I. INTRODUCTION

IN spite of the importance of the subject, little theoretical work has been done on the dynamics of dislocations in crystals from a discrete, microscopic

viewpoint. The earliest work on two-dimensional dislocation dynamics considered a single volterra dislocation in an infinite elastic continuum; in this model the dislocation may move freely at any velocity less than the speed of sound without an applied stress.<sup>1</sup> A similar solution was found<sup>2,3</sup> for a modified continuum

\* This research was supported by the U. S. Air Force through the Air Force Office of Scientific Research under Contract No. AF-AFOSR-(228)-63.

† Currently NAS-NRC Postdoctoral Fellow at Institute for Materials Research, National Bureau of Standards, Washington, D. C.

<sup>1</sup> F. C. Frank, Proc. Phys. Soc. (London) **A62**, 131 (1949).

<sup>2</sup> J. D. Eshelby, Proc. Phys. Soc. (London) **A62**, 307 (1949).

<sup>3</sup> R. Bullough and B. A. Bilby, Proc. Phys. Soc. (London) **B67**, 615 (1954).

model proposed by Peierls<sup>4,5</sup>: In order to account for the periodicity of the lattice and the resulting variation in lattice strain energy as the dislocation passes from one equilibrium position to the next, opposing atoms on the slip plane were assumed subject to a periodic sinusoidal restoring force, the rest of the crystal above and below the slip plane being taken as elastic and continuous.

In order to develop a relationship between applied stress and dislocation velocity, an energy-loss mechanism must be postulated. This question has been recognized as quite important, and some of the work is summarized with further references to the literature by Cottrell<sup>6</sup> and Seeger.<sup>7</sup> A critique of earlier estimates of energy loss along with calculations resulting in much higher values than the earlier estimates is given by Kuhlmann-Wilsdorf.<sup>8</sup> The loss mechanisms considered include the effects of thermal motion of the lattice, of other lattice defects, and of the discrete nature of the lattice. The last effect is the subject of the present work. Because of the complexity of the problem it is clear that any atomistic treatment must of necessity be based upon a highly idealized model. Nevertheless, such treatments provide insights into the nature of the processes which may then be incorporated in more phenomenological models. An added incentive for analysis in this area has been provided by development of experimental techniques by Johnston and Gilman<sup>9</sup> for the measurement of individual dislocation velocities in crystals.

Much recent work has concentrated on one-dimensional linear-chain models because these may be treated in greater detail with fewer assumptions. A discussion of the Peierls model and earlier work on linear-chain models is given by Seeger,<sup>7</sup> Atkinson and Cabrera,<sup>10</sup> taking issue with the continuous approximations made in the dynamic analyses of some of the previous work, treat a linear chain from a discrete viewpoint.

In a recent paper, Weiner<sup>11</sup> has presented an approximate analytical procedure for the computation of dislocation velocities in a linear chain of atoms. In this approach successive states of the dislocation, referred to as stable and unstable, are distinguished. In each state the atom velocities in the neighborhood of the dislocation are approximated by use of the appropriate localized normal mode of motion of the chain. It is found, for the atoms of the chain under an applied stress, that steady-state dislocation velocities are attained because of the imperfect transfer of energy

between successive localized modes. Computer simulation of the linear chain showed that the localized-mode approximation was reasonably accurate except for dislocation velocities approaching the speed of wave propagation for infinite wavelength in the infinite chain. It is the purpose of the present work to extend the localized-mode approach to a two-dimensional crystal model.

The model studied is similar to that employed by Sanders<sup>12</sup> in his treatment of the static Peierls stress. However, for the present dynamic calculations a further simplification of Sanders' model is made by replacing the effects of the crystal below the slip plane by a time-independent substrate potential. The resulting model is described in Sec. II. Also contained in this section are the analyses of the static configuration of this model which are necessary preliminary to the dynamic calculations. Particular attention is paid to the determination of the characteristics of the stable and unstable equilibrium configurations. One surprising result is that, as opposed to the results for the linear chain, there is no localized mode (localized normal mode of vibration) associated with the stable equilibrium configuration of this two-dimensional model. However, there is a localized mode associated with the unstable equilibrium configuration.

In Sec. III a dynamic analysis is made based on the following assumptions: (1) The motion of the dislocation while the lattice is in an unstable configuration is essentially given by the localized mode associated with this configuration<sup>13</sup>; (2) the motion of the dislocation while the lattice is in a stable configuration may be represented by the above-mentioned localized mode altered so that it is symmetric with respect to the stable equilibrium configuration. As in the linear chain, it is found that there is imperfect transfer of energy between modes. Transient and steady-state velocities and the minimum stress needed to sustain motion are then calculated.

Finally, numerical calculations on a finite lattice using the IBM-7094 computer are made. A detailed discussion of the theoretical and numerical results is presented in Sec. V.

## II. MODEL DESCRIPTION AND STATIC ANALYSIS

A Rosenstock-Newell crystal lattice, simple-cubic with atomic spacing  $b$  and central and noncentral

<sup>4</sup> R. Peierls, Proc. Phys. Soc. (London) **52**, 34 (1940).

<sup>5</sup> F. R. N. Nabarro, in *Advances in Physics*, edited by N. F. Mott (Taylor and Francis, Ltd., London, 1952), Vol. 1, p. 269.

<sup>6</sup> A. H. Cottrell, *Dislocations and Plastic Flow in Crystals* (Clarendon Press, Oxford, England, 1953), p. 56.

<sup>7</sup> A. Seeger, in *Handbuch der Physik*, edited by S. Flügge (Springer-Verlag, Berlin, 1956), Vol. VII/1, 563.

<sup>8</sup> D. Kuhlmann-Wilsdorf, Phys. Rev. **120**, 773 (1960).

<sup>9</sup> W. G. Johnston and J. J. Gilman, J. Appl. Phys. **30**, 129 (1959).

<sup>10</sup> W. Atkinson and N. Cabrera, Phys. Rev. **138**, A763 (1965).

<sup>11</sup> J. H. Weiner, Phys. Rev. **136**, A863 (1964).

<sup>12</sup> W. T. Sanders, Phys. Rev. **128**, 1540 (1962).

<sup>13</sup> It has been noted [H. B. Rosenstock and C. C. Klick, Phys. Rev. **119**, 1198 (1960)] that the contribution to the relative atomic displacements near the point of localization of the localized mode, of the large number of nonlocalized modes, taken together, may be of the same order of magnitude as that of the localized mode. The results of previous work (Ref. 11), however, indicate that the localized mode may nevertheless provide a good approximation for the directed, athermal motion of the dislocation under consideration here; the nonlocalized-mode contributions, on the other hand, are important in the study of thermal effects upon this motion [J. H. Weiner, Phys. Rev. **139**, A442 (1965)].

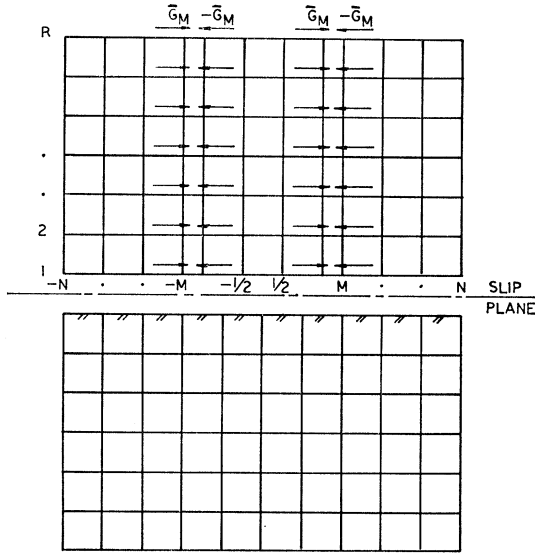


FIG. 1. Reference position for displacements due to the introduction of an edge dislocation into a simple-cubic lattice. The atoms below the slip plane are fixed. The forces  $\mathbf{G}_M$  were applied after the crystal had been separated along the slip plane and an extra half-plane of atoms introduced into the upper half, so that the atoms ( $|j| \geq M$ ) on the slip plane would align when the crystal was brought together again.

linear interactions of spring constant  $k_1$  and  $k_2$ , respectively, is used.<sup>12</sup>

An edge dislocation is introduced by the following procedure: The crystal is separated along the slip plane and an extra plane of atoms introduced into the upper half. Two columns are chosen from the center of the upper half, and labelled  $-M$  and  $M$  (Fig. 1). To each atom of column  $-M$  a force  $\mathbf{G}_M$  given by Eq. (2.1) is applied and to each atom of column  $M$  a force  $-\mathbf{G}_M$ :

$$|\mathbf{G}_M| = \frac{1}{2}k_1b. \quad (2.1)$$

Forces  $-\mathbf{G}_M$ ,  $\mathbf{G}_M$  are applied to the columns  $-M+1$  and  $M-1$ , respectively. The result is shown in Fig. 1. If there are an odd number of columns between  $-M$  and  $M$ , the central column is labeled 0; if an even number, the central pair of columns is labeled  $-\frac{1}{2}$  and  $\frac{1}{2}$ . All other column indices increase by 1 per column from  $-N$  to  $N$ .  $M$  is thus either an integer or a half odd integer. It characterizes the width of the dislocation in that all slip-plane atoms for which  $|j| \geq M$  are directly opposite atoms in the lower half, while the others are out of register by  $\frac{1}{2}b$ . The row index  $i$  ranges from 1 to  $R$ .

The halves are brought together. The atoms of the lower half are fixed and their effect on the upper half replaced by a periodic substrate potential  $U(\zeta)$  acting on the slip-plane atoms of the upper half, where

$$U(\zeta) = \frac{1}{2}k_2\zeta^2, \quad |\zeta| \leq \phi, \quad (2.2)$$

$$U(\zeta) = \frac{1}{2}k_2\phi b - k_2\phi(b-2\phi)^{-1}(\frac{1}{2}b-\zeta)^2, \quad \phi \leq |\zeta| \leq \frac{1}{2}b, \quad (2.3)$$

and  $\zeta$  is the distance from a potential minimum. The force law corresponding to this potential is shown in Fig. 2. Thus, the atoms of the slip plane are connected to a fixed boundary by springs with spring constant  $k_2$  for  $|j| \geq M$  and  $-2k_2\phi/(b-2\phi)$  for  $|j| < M$ . The former atoms are said to have strong bonds with the substrate potential, the latter atoms weak bonds with the substrate potential. Finally, the forces  $\mathbf{G}_M$  are released.

Lattice configurations with one weak bond and with two weak bonds,  $M=1$  and  $M=\frac{3}{2}$ , will be considered in this paper.

### Static Displacements

The displacement in the  $x$  direction of the atom in row  $i$  column  $j$  from the reference position of Fig. 1 is denoted by  $u_{ij}$ . It has a symmetric ( $u_{ij}^\sigma = u_{i,-j}^\sigma$ ) component resulting from the application of the external shear force  $\bar{\sigma}$  per atom and an antisymmetric ( $u_{i,-j}^\sigma = -u_{i,j}^\sigma$ ) component resulting from the removal of the forces  $\mathbf{G}_M$ . At large distances from the dislocation the symmetric displacements must approach the uniform shear  $i\bar{\sigma}/k_2$ . If the displacements are reduced by this amount ( $\bar{u}_{ij} = u_{ij} - i\bar{\sigma}/k_2$ ) and the resulting equations divided through by  $k_1b$  ( $u_{ij} = \bar{u}_{ij}/b$ ) to put them in dimensionless form, the equations of equilibrium for one weak bond in terms of antisymmetric and symmetric components become

$$u_{i,j-1}^\sigma - (2+2P)u_{ij}^\sigma + u_{i,j+1}^\sigma + Pu_{i-1,j}^\sigma + Pu_{i+1,j}^\sigma = -\frac{1}{2}\delta_{j1} + \frac{1}{2}\delta_{j,-1}, \quad (2.4)$$

$$u_{0j}^\sigma = 0, \quad \lim_{|j| \rightarrow \infty} u_{ij}^\sigma = 0,$$

$$u_{i,j-1}^\sigma - [(2+2P) - (P+Q)\delta_{i1}\delta_{j0}]u_{ij}^\sigma + u_{i,j+1}^\sigma + Pu_{i-1,j}^\sigma + Pu_{i+1,j}^\sigma = \delta_{j0}\delta_{i1}(P+Q)\sigma, \quad (2.5)$$

$$u_{0j}^\sigma = 0, \quad \lim_{i \rightarrow \infty} u_{ij}^\sigma = 0, \quad \lim_{|j| \rightarrow \infty} u_{ij}^\sigma = 0,$$

where  $\delta_{ij}$  is the Kronecker delta. Here and in what follows, the summation convention on repeated latin indices is employed.

$$P = k_2/k_1, \quad \gamma = \phi/b, \quad Q = 2\gamma P/(1-2\gamma). \quad (2.6)$$

The solutions are found by multiplying the equations by  $z^j$ , summing over  $j$ , and introducing the new variable (see Babuška *et al.*<sup>14</sup> and Sanders<sup>12</sup>):

$$\bar{u}_i^{\sigma,\sigma} = \sum_{j=-\infty}^{\infty} u_{ij}^{\sigma,\sigma} z^j, \quad |z| = 1. \quad (2.7)$$

This is a valid procedure provided

$$\lim_{|j| \rightarrow \infty} u_{i,j}^{\sigma,\sigma} = 0.$$

<sup>14</sup> I. Babuška, E. Vitasek, and F. Kroupa, Czech. J. Phys. 10, 488 (1960).

The resulting difference equations in the variable  $\bar{u}_i^{a,\sigma}$  may be solved by a solution of the form  $\bar{u}_i^{a,\sigma} = A^{a,\sigma}\beta^i + B^a$ , where  $A^{a,\sigma}$ ,  $\beta$ , and  $B^a$  are determined by direct substitution in the equations. The coefficients in the Laurent expansion, Eq. (2.7), are then given by

$$2\pi u_{ij}^{a,\sigma} \sqrt{-1} = \oint \bar{u}_i^{a,\sigma} z^{-j-1} dz, \quad |z|=1. \quad (2.8)$$

An identical procedure leads to the displacements of the two-weak-bond configuration; only the antisymmetric displacements are of interest. The general solutions for the static displacements in integral form, along with specific displacements needed further on in the development, are

for one weak bond

$$4\pi u_{ij}^a = P^{-i} \int_0^{2\pi} \sin\theta (1 - \cos\theta)^{-1} (P^i - E^i) \times \sin(j\theta) d\theta, \quad (2.9)$$

$$4\pi P u_{11}^a = 2(1-P)P^{1/2} + (1+P)^2 G - \pi, \quad (2.10)$$

$$2\pi u_{ij}^\sigma = (P+Q)(u_{10}^\sigma + \sigma) P^{-i-1} \times \int_0^{2\pi} E^i \cos(j\theta) d\theta, \quad (2.11)$$

$$u_{10}^\sigma = \sigma H / (\pi P^2 - H), \quad (2.12)$$

$$2\pi P^2 u_{11}^\sigma = (P+Q)(u_{10}^\sigma + \sigma) [2(1+P)P^{1/2} + (1+2P)(1-P)G - \pi], \quad (2.13)$$

and for two weak bonds,

$$2\pi u_{ij}^a = \int_0^{2\pi} \{ [2u_{1,\frac{1}{2}}^a (P+Q)P^{-1} - K] E^i - K \} \times \sin(\frac{1}{2}\theta) \sin(j\theta) d\theta, \quad (2.14)$$

$$u_{1,\frac{1}{2}}^a = P \left[ \frac{1}{2}\pi - (1+P)P^{1/2} + (P^2 - 1)G \right] \div \{ 2\pi P^2 - 2(P+Q) \left[ \left( \frac{3}{2} + P \right) \pi - (3+P)P^{1/2} - \frac{1}{2}(3-P)(1+P)G \right] \}, \quad (2.15)$$

where

$$\begin{aligned} E &= 1 + P - \cos\theta - [(1 - \cos\theta)(1 + 2P - \cos\theta)]^{1/2}, \\ G &= \frac{1}{2}\pi + \arcsin[(1 - P)/(1 + P)], \\ H &= (P + Q)[(1 + P)(\pi - G) - 2P^{1/2}], \\ K &= [1 - 2\sin^2(\frac{1}{2}\theta)](1 - \cos\theta)^{-1}. \end{aligned}$$

Application of the Riemann-Lebesgue lemma<sup>15</sup> verifies that

$$\lim_{|j| \rightarrow \infty} u_{ij}^{a,\sigma} = 0.$$

The displacement equations of equilibrium were solved under the assumption that the displacements of atoms on the slip plane were less than  $\phi$  for all atoms

<sup>15</sup> H. S. Carslaw, *Introduction to the Theory of Fourier's Series and Integrals* (Dover Publications, New York, 1930), p. 271.

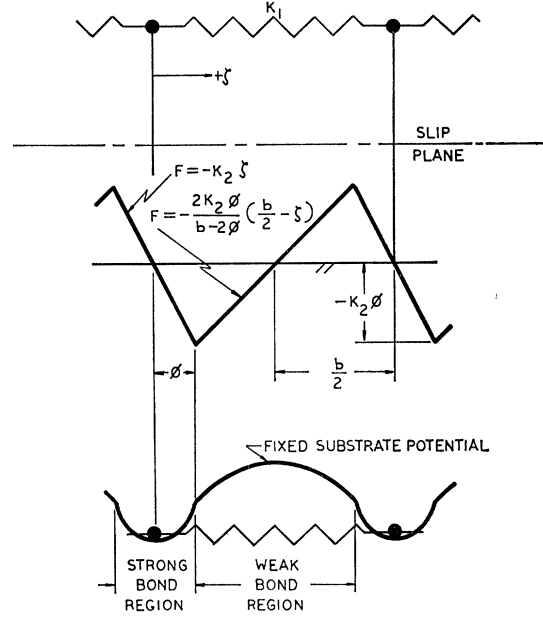


FIG. 2. Force law for atoms on the slip plane and the corresponding substrate potential. The slope of the potential curve in this and Fig. 4 is shown as discontinuous to more clearly distinguish weak- and strong-bond regions.

on the slip plane except the weakly bonded ones and less than  $\frac{1}{2}b - \phi$  for the latter. That this is indeed so places a requirement on the solution here termed compatibility. With  $\gamma$  chosen such that a one-weak-bond configuration is stable and compatible and a two-weak-bond configuration is unstable, it can be shown that the latter must also be compatible. Compatibility is established for one weak bond if the following inequalities are satisfied:

$$u_{11}^a < \gamma, \quad (2.16)$$

$$u_{1,j+1}^a < u_{1,j}^a, \quad |j| \geq 1, \quad (2.17)$$

$$u_{1,j+1}^\sigma < u_{1,j}^\sigma, \quad |j| \geq 1, \quad (2.18)$$

$$u_{11}^a + u_{11}^\sigma + \sigma < \gamma, \quad (2.19)$$

$$u_{10}^\sigma + \sigma < \frac{1}{2} - \gamma. \quad (2.20)$$

The first inequality gives the compatibility limit on  $\gamma$ ; with  $u_{11}^a$  given by Eq. (2.10) it becomes

$$4\pi\gamma P > 2(1-P)P^{1/2} + (1+P)^2 G - \pi. \quad (2.21)$$

Inequalities (2.17) and (2.18) follow from Eq. (2.8). The largest value of  $\sigma$  for which both of the last two inequalities are satisfied is the largest  $\sigma$  which the lattice can sustain in static equilibrium; it is therefore the Peierls stress  $\sigma_P$  for this model. For  $P=1$  and after substitution from Eqs. (2.10), (2.12), and (2.13) these inequalities become

$$\sigma < 2(\gamma - \frac{1}{4})[2(1+Q) - Q\pi] \times [8(1+Q) - (1+3Q)\pi]^{-1}, \quad (2.22)$$

$$\sigma < \pi^{-1}(\frac{1}{2} - \gamma)[2(1+Q) - Q\pi]. \quad (2.23)$$

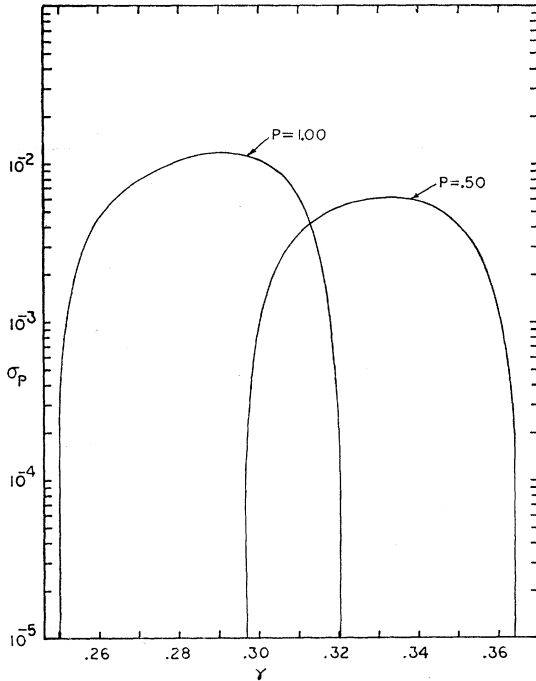


FIG. 3. Variation of the maximum shear stress  $\sigma_P$  (Peierls stress) the lattice can sustain, with the maximum force  $\gamma$  an atom on the slip plane can experience due to the substrate potential.

The second is satisfied if the first is, so that for  $P=1$  the Peierls stress  $\sigma_P$  is given by Eq. (2.22) with the inequality replaced by equality. The Peierls stress for various  $P$  and  $\gamma$  is shown in Fig. 3; it is given by Sanders<sup>12</sup> for the complete two-dimensional model and by Weiner and Sanders<sup>16</sup> for the linear chain.

### Stability

An atom in the lattice experiences a force due to interaction with its neighbors of  $-\Phi_{ijk}\tilde{q}_{kl}$ , where  $\Phi_{ijk}$  is the potential matrix ( $\tilde{q}_{ij}\Phi_{ijk}\tilde{q}_{kl}$  is the potential energy of the lattice) and  $\tilde{q}_{ij}$  are the displacements from equilibrium. Then the equations of motion are

$$\Phi_{ijk}\tilde{q}_{kl} + m(d^2/dt^2)\tilde{q}_{ij} = 0. \quad (2.24)$$

A solution for which all displacements are proportional to the same periodic function of time is

$$\tilde{q}_{ij} = \bar{q}_{ij} \exp(-m\lambda/k_1)t^{1/2};$$

if this is substituted into Eq. (2.24) and the result divided by  $k_1 b$  it becomes

$$-\Phi_{ijk}q_{kl} + \lambda q_{ij} = 0, \quad (2.25)$$

where

$$\Phi_{ijk}/k_1 = \Phi_{ijk}, \quad \tilde{q}_{ij}/b = q_{ij}.$$

The values of  $\lambda$  for which this system has a solution constitute the frequency, or eigenvalue, spectrum and

<sup>16</sup> J. H. Weiner and W. T. Sanders, Phys. Rev. 134, A1007 (1964).

the corresponding  $q_{ij}$  the normal modes of vibration, or eigenvectors, of the lattice. If any of the eigenvalues are negative, the general solution contains an increasing time exponential and the lattice is unstable. If the lattice parameters are now altered at some point such that the potential energy of a given configuration is reduced, as is the case when weak bonds are introduced, all the eigenvalues will be lowered<sup>17</sup>; some may be displaced below the original perfect lattice spectrum and then their corresponding eigenvector is localized.<sup>18</sup> If no localized eigenvector exists, the lowest eigenvalue (the criterion for stability) is equal to that of the perfect lattice.

For the finite perfect lattice with fixed boundaries Eq. (2.25) is

$$q_{i,j-1} - (2+2P)q_{ij} + q_{i,j+1} + Pq_{i-1,j} + Pq_{i+1,j} = 0, \quad (2.26)$$

$$q_{0j} = q_{R,j} = q_{-Nj} = q_{Nj} = 0, \quad (2.27)$$

with a solution, found by the separation of variables  $q_{ij} = x^i y^j$ ,

$$\lambda^{\alpha\beta} = 2 + 2P - 2 \cos[(\beta + \frac{1}{2})\pi/N] - 2P \cos(\alpha\pi/R), \quad (2.28)$$

$$\begin{cases} \alpha = 1, 2, \dots, R-1 \\ \beta = 0, 1, 2, \dots, N-1 \end{cases}$$

$$q_{ij}^{\alpha\beta} = A \sin(\alpha\pi i/R) \cos[(\beta + \frac{1}{2})\pi j/N]. \quad (2.29)$$

As the lattice becomes infinite the  $\lambda^{\alpha\beta}$  approach a continuous spectrum from 0 to  $4(1+P)$ . Thus instability can only be introduced by a mode with frequency below the continuous band, i.e., by a localized mode; the absence of a localized mode guarantees stability. It is characteristic of a localized mode that  $\lim_{|j| \rightarrow \infty} q_{ij} = 0$ , so that if a localized mode does exist it may be found by the transform technique  $\tilde{q}_i = \sum_{-\infty}^{\infty} q_{ij} z^j$  applied to Eq. (2.25) which, along with its eigenvector (localized-mode) solution and corresponding eigenvalue equation for one weak bond is

$$q_{i,j-1} - [2 + 2P - (P+Q)\delta_{i1}\delta_{j0} - \lambda]q_{ij} + q_{i,j+1} + Pq_{i+1,j} + Pq_{i-1,j} = 0, \quad (2.30)$$

$$q_{0j} = 0, \quad \lim_{|j| \rightarrow \infty} q_{ij} = 0,$$

$$2\pi q_{ij} = q_{10}(P+Q)P^{-i-1}$$

$$\times \int_0^{2\pi} [1 + P - \frac{1}{2}\lambda - \cos\theta - L]^i \cos(j\theta) d\theta, \quad (2.31)$$

$$2\pi\gamma P = \int_0^\pi L d\theta + \frac{1}{2}\lambda - 1, \quad (2.32)$$

<sup>17</sup> Lord Rayleigh, *The Theory of Sound* (Dover Publications, New York, 1945), Vol. I, p. 111.

<sup>18</sup> A. A. Maradudin, E. W. Montroll, and G. H. Weiss, in *Solid State Physics*, edited by F. Seitz and D. Turnbull (Academic Press Inc., New York, 1963), Suppl. 3, p. 129.

and for two weak bonds,

$$q_{i,j-1} - [2 + 2P - (P+Q)(\delta_{i1}\delta_{j,-\frac{1}{2}} + \delta_{i1}\delta_{j,\frac{1}{2}}) - \lambda]q_{ij} \\ + q_{i,j+1} + Pq_{i-1,j} + Pq_{i+1,j} = 0, \quad (2.33) \\ q_{0j} = 0, \quad \lim_{|j| \rightarrow \infty} q_{ij} = 0,$$

with a symmetric solution

$$\pi q_{ij}^\sigma = q_{1,\frac{1}{2}}^\sigma (P+Q)P^{-i-1} \int_0^{2\pi} \cos(\frac{1}{2}\theta) \\ \times (1 + P - \frac{1}{2}\lambda - \cos\theta - L)^i \cos(j\theta) d\theta, \quad (2.34)$$

$$2\pi\gamma P = \int_0^\pi (1 + \cos\theta)L d\theta + \frac{1}{2}\lambda - \frac{1}{2}, \quad (2.35)$$

and an antisymmetric solution

$$\pi q_{ij}^\alpha = q_{1,\frac{1}{2}}^\alpha (P+Q)P^{-i-1} \int_0^{2\pi} \sin(\frac{1}{2}\theta)L^i \sin(j\theta) d\theta, \quad (2.36)$$

$$2\pi\gamma P = \int_0^\pi (1 - \cos\theta)L d\theta + \frac{1}{2}\lambda - \frac{3}{2}, \quad (2.37)$$

where

$$L = [(1 - \frac{1}{2}\lambda - \cos\theta)(1 + 2P - \frac{1}{2}\lambda - \cos\theta)]^{1/2}.$$

The eigenvalue equations (2.32) (for one weak bond) (2.35) and (2.37) (for two weak bonds) come from the requirement that the expressions for the corresponding eigenvectors be consistent for  $i, j=1, 0$  (for 1 weak bond) and  $i, j=1, \frac{1}{2}$  (for 2 weak bonds); as was to be expected, they have no solution for positive  $\lambda$ . Let  $\gamma_1, \gamma_2$ , and  $\gamma_3$ , respectively, satisfy Eqs. (2.32), (2.35), and (2.37) for  $\lambda=0$ . By Rayleigh's theorems, since the weak-bond spring constant decreases (and therefore all the eigenvalues decrease) with an increase in  $\gamma$ , these are the minimum values of  $\gamma$  for which the eigenvalue equations have a solution and therefore for which a localized mode exists. Representative values of  $P, \gamma_1, \gamma_2$ , and  $\gamma_3$  follow:

$P$	$\gamma_1$	$\gamma_2$	$\gamma_3$
0.5	0.362	0.297	0.430
1	0.318	0.250	0.387
2	0.269	0.203	0.335

It will be noted that  $\gamma_3 > \gamma_1$ . It follows that for  $\gamma_2 < \gamma < \gamma_1$ , the configuration with one weak bond will be stable with no localized mode and the configuration with two weak bonds will be unstable, with a single symmetric localized mode. The eigenvector, Eq. (2.36), corresponding to this mode may be normalized,  $q_{ij}q_{ij} = 1$ , by applying Parseval's theorem<sup>19</sup> to the  $j$  summation and then summing over  $i$ . Then

$$q_{1,\frac{1}{2}}^2 (P+Q)^2 \left[ \int_0^\pi \cos^2(\frac{1}{2}\theta) (R+R^{-1}) d\theta - \pi \right] = \pi P^2, \quad (2.38)$$

<sup>19</sup> Reference 15, p. 284.

where

$$R = (1 - \frac{1}{2}\lambda - \cos\theta)^{1/2} (1 + 2P - \frac{1}{2}\lambda - \cos\theta)^{-1/2}. \quad (2.39)$$

Finally, the inequality  $\gamma > \gamma_2$  is seen to be identical with Eq. (2.21), so that compatibility is also satisfied.

### III. DYNAMIC ANALYSIS

The velocity of the dislocation will now be investigated under the assumption that no thermal motion of the atoms takes place. The dislocation is assumed to move through alternating stable and unstable configurations which have one and two weak bonds, respectively. Because the displacements of the atoms far from the dislocation are essentially those of a perfect lattice under a quasistatic application of shear, with respect to which the dislocation is moving in a localized fashion, the equations of motion will be written in terms of displacements  $\bar{v}_{ij}$  from the zero-stress equilibrium configuration that are reduced by the quasistatic shear displacement,  $i\bar{\sigma}/k_2$ . The displacement at any time  $t$  is then  $\bar{u}_{ij}^\alpha + i\bar{\sigma}/k_2 + \bar{v}_{ij}(t)$ . If  $\bar{F}_{ij}$  is the force on the  $i, j$ th atom, the equations of motion for  $\bar{v}_{ij}(t)$  are

$$-\bar{\Phi}_{ijkil}\bar{v}_{kl} + \bar{F}_{ij} = m(d^2/dt^2)\bar{v}_{ij}. \quad (3.1)$$

Division by  $k_1b$  and introduction of the dimensionless time  $t = (k_1/m)^{1/2}t$  and displacement  $v_{ij} = \bar{v}_{ij}/b$  gives

$$-\Phi_{ijkil}v_{kl} + F_{ij} = \ddot{v}_{ij}. \quad (3.2)$$

The left-hand side as a function of  $v_{kl}$  is given by the equations of equilibrium. In the following, quantities referring to the stable or unstable lattice will be distinguished by the superscripts  $S$  or  $U$ .

For the choice of parameters made in Sec. II there exists an unstable localized symmetric mode of vibration whose components are small everywhere except in the neighborhood of the dislocation. Only one such mode exists, because altering the one-weak-bond lattice by reducing a single spring constant to produce a two-weak-bond lattice permits only one frequency to be displaced out of the originally continuous spectrum. This is a consequence of Rayleigh's theorem,<sup>17</sup> which states that under these circumstances no frequency can be lowered more than the distance to the next lowest unperturbed frequency. Thus, all frequencies except the lowest are obliged to remain within the original spectrum. The closure property<sup>20,21</sup> of the eigenvectors of a symmetric matrix then assures that in the neighborhood of the dislocation the components of all eigenvectors except the localized one will be small. The displacement in the neighborhood of the dislocation, when the lattice is unstable, may therefore be approximated by<sup>13</sup>

$$v_{ij}^U = a_{ij}^U Q^U(t), \quad Q^U(t) = a_{ij}^U v_{ij}^U, \quad (3.3)$$

<sup>20</sup> R. L. Bjork, Phys. Rev. **105**, 456 (1957).

<sup>21</sup> J. A. Krumhansl, J. Appl. Phys. Suppl. **33**, 307 (1962).

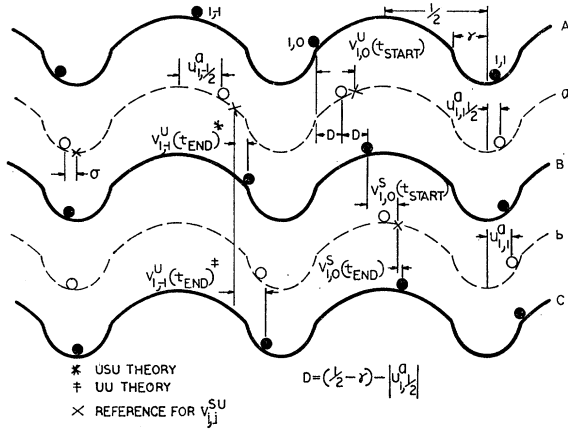


FIG. 4. Progress of the atoms on the slip plane. In (A) an unstable traverse is about to start; it ends in (B) and a stable traverse starts which ends in (C), thus completing a dislocation move of 1 atomic spacing. The zero-stress unstable- and stable-equilibrium configurations are shown in (a) and (b); at a distance  $\sigma$  to the right of these is the reference position for dynamic displacements. Dynamic displacements are shown for those atoms whose position at the time of change is used to determine the value of the normal coordinate at that instant.

where  $a_{ij}^U$  is the localized eigenvector and  $Q^U$  the corresponding normal coordinate;  $a_{ij}^U$  is given by Eq. (2.36) provided the arbitrary component  $q_{1,3}$  is chosen, Eq. (2.38), so as to normalize  $q_{ij}$ . It is convenient to let  $a_{ij}^U$  have integer subscripts,  $a_{1,-3}^U = a_{1,-1}^U$ ,  $a_{1,3}^U = a_{1,0}^U$ , etc.

The potential matrices of a stable and unstable lattice differ in only one term. Furthermore, at the instant the lattice becomes stable, the motion of the atoms in the neighborhood of the dislocation is given by the unstable localized mode. It seems reasonable to make use of the unstable localized mode in approximating the solution to the equations of stable dislocation motion. However, the change to a stable configuration alters the lattice symmetry. A simple form of localized stable motion, symmetric with respect to the stable lattice, may then be described by the vector

$$a_{ij}^S = A(a_{ij}^U + a_{i,j-1}^U). \quad (3.4)$$

From the requirement that  $a_{ij}^S a_{ij}^S = 1$  it follows that

$$A = [2(1 + a_{ij}^U a_{i,j-1}^U)]^{-1/2}.$$

The sum  $a_{ij}^U a_{i,j-1}^U$  is found by using a Fourier cosine series approach to sum over  $j$ . Then

$$\pi P^2 a_{ij}^U a_{i,j-1}^U = q_{1,3}^2 (P+Q)^2 \left[ \int_0^{2\pi} W^{-j} \cos\theta \cos^2(\frac{1}{2}\theta) d\theta + \int_0^{2\pi} W \cos\theta \cos^2(\frac{1}{2}\theta) d\theta - \frac{1}{2}\pi \right], \quad (3.5)$$

where

$$W = [(1 + 2P - \cos\theta - \frac{1}{2}\lambda U) / (1 - \cos\theta - \frac{1}{2}\lambda U)]^{1/2}.$$

The displacements corresponding to  $a_{ij}^S$  are

$$v_{ij}^S = Q^S(t) a_{ij}^S, \quad Q^S(t) = a_{ij}^S v_{ij}^S. \quad (3.6)$$

The approximations  $v_{ij}^U = a_{ij}^U Q^U$  and  $v_{ij}^S = a_{ij}^S Q^S$  are substituted into the equations of motion (3.2). With the use of the following relations,

$$\begin{aligned} \Phi_{ijkl}^U a_{kl}^U &= \lambda^U a_{ij}^U, \\ F_{ij}^U &= (P+Q)\sigma(\delta_{j0} + \delta_{j1})\delta_{i1}, \\ F_{ij}^S &= (P+Q)\sigma\delta_{j0}\delta_{i1}, \\ \Phi_{ijkl}^S &= \Phi_{ijkl}^U + (P+Q)\delta_{i1}\delta_{j,-1}\delta_{k1}\delta_{l,-1} \\ &= \Phi_{i,j-1,k,l-1} + (P+Q)\delta_{i1}\delta_{j1}\delta_{k1}\delta_{l1}, \end{aligned} \quad (3.7)$$

the equations of motion for  $Q^{U,S}$  become

$$\ddot{Q}^U + \lambda^U Q^U = F_U, \quad (3.8)$$

$$\ddot{Q}^S + [\lambda^U + (P+Q)a_{10}^U(a_{10}^U + a_{11}^U)]Q^S = F_S, \quad (3.9)$$

where

$$F_U = 2a_{10}^U(P+Q)\sigma,$$

$$F_S = \sqrt{2}a_{10}^U(P+Q)(1 + a_{i,j}a_{i,j-1})^{-1/2}\sigma.$$

Now that the motion during unstable and stable periods has been approximated by means of the coordinates  $Q^S$  and  $Q^U$ ; they will be used to form a picture of the continuous motion of the dislocation through the lattice. This requires the determination of the initial and final values of  $Q^{U,S}$  and the relation between  $\dot{Q}^U$  and  $\dot{Q}^S$  when going from a stable to unstable lattice, or vice versa.

The localized vector  $a_{ij}^S$  is not a true eigenvector of the stable lattice (which, as was shown, has no localized eigenvector); its use coarsens the theory somewhat and so it is of interest to examine the situation when the unstable mode predominates, that is, its time of traverse is large compared to that of the stable mode. In this case it is assumed that the motion is described by the unstable mode even in the stable configuration, since the latter does not exist long enough to affect the pattern of motion. This special case is called *UU* motion; the general case, *USU* motion.

### USU Motion

Let the periods of alternately stable and unstable motion be  $t_k$  to  $t_{k+1}$ ,  $k$  even giving the stable period and  $k$  odd the unstable period. Initially,  $t_0$ , the lattice is in a state of uniform shear strain,  $v_{ij}^U = u_{ij}^a + i\sigma$ . Uniform shear is not an equilibrium configuration for the dislocation distorted lattice and so the dislocation starts to move. The values of  $Q^{U,S}$  at the start and end of a traverse may be found from Eqs. (3.3) and (3.6) if one of the  $v_{ij}^{U,S}$  are known at the time of transition. The situation is shown in Fig. 4 for the weak-bond atoms at 1, 0 and 1, -1. From Fig. 4

$$\begin{aligned} Q^U(t_k) &= v_{10}^U(t_{\text{START}})/a_{10}^U \\ &= -(\frac{1}{2} - \gamma + U_{1,3}^a + \sigma)/a_{10}^U \equiv -dL_U, \end{aligned} \quad (3.10)$$

$$\begin{aligned} Q^U(t_{k+1}) &= v_{1,-1}^U(t_{\text{END}})/a_{1,-1}^U \\ &= (\frac{1}{2} - \gamma + U_{1,3}^a - \sigma)/a_{10}^U \equiv dR_U, \end{aligned} \quad k \text{ even}, \quad (3.11)$$

$$Q^S(t_k) = v_{1,0}^S(t_{\text{START}})/a_{10}^S \\ = -(2|U_{1,1}^S| + \gamma - \frac{1}{2} + \sigma)/a_{10}^S \equiv -dL_S, \quad (3.12)$$

$$Q^S(t_{k+1}) = v_{1,0}^S(t_{\text{END}})/a_{10}^S \\ = (2|U_{1,1}^S| + \gamma - \frac{1}{2} - \sigma)/a_{10}^S \equiv dR_S, \quad (3.13)$$

$k \text{ odd.}$

These values do not change with dislocation position.

At any time  $t$  the coordinates  $v_{ij}^S$  and  $v_{ij}^U$  differ only in their fixed references, so that at some particular unstable to stable transition  $\dot{v}_{ij}^{S'}(t_k) = \dot{v}_{ij}^{U'}(t_k)$ . From this and Eqs. (3.3) and (3.6)

$$\dot{Q}^{S'}(t_k) = a_{ij}^S a_{ij}^{U'} \dot{Q}^{U'}(t_k). \quad (3.14)$$

At  $t_{k+1}$  the weakly bonded atoms change from 1,  $j_w$  to 1,  $j_w$  and 1,  $j_w+1$ . In this case, with  $U''$  denoting the new unstable position,

$$\dot{Q}^{U''}(t_{k+1}) = a_{ij}^{U''} a_{ij}^{S'} \dot{Q}^{S'}(t_{k+1}), \quad k \text{ odd.} \quad (3.15)$$

Though the subscripts change, the localized vectors are always centered with respect to the present position of the dislocation—that is,

$$a_{ij}^{U'} = a_{i,j-j_w}^U, \quad a_{ij}^{S'} = a_{i,j-j_w}^S, \quad a_{ij}^{U''} = a_{i,j+1}^{U'}.$$

It follows that

$$a_{ij}^{S'} a_{ij}^{U'} = a_{ij}^{U''} a_{ij}^{S'} = a_{ij}^U a_{ij}^S \equiv B < 1. \quad (3.16)$$

The symmetry of the localized vectors thus leads to velocity transfers which are the same for stable to unstable and unstable to stable, namely,

$$\dot{Q}^S(t_k) = B^{1/2} \dot{Q}^U(t_k), \quad k \text{ odd}, \quad (3.17)$$

$$\dot{Q}^U(t_k) = B^{1/2} \dot{Q}^S(t_k), \quad k \text{ even}. \quad (3.18)$$

Dislocation motion is now completely characterized by the coordinates  $Q^{S,U}$ , which may be thought of as describing the motion of a series of alternating stable and unstable asymmetric pendulums, each subjected to a constant force and imperfectly transferring energy from one to the next. This interpretation is illustrated in Fig. 5. Let

$$\omega_U^2 = |\lambda^U|, \quad \omega_S^2 = \lambda^U + (P+Q)a_{10}^U(a_{10}^U + a_{11}^U) / \\ (1 + a_{ij}^U a_{i,j-1}^U), \quad (3.19)$$

$$\Delta U = 2F_U(dR_U + dL_U)\sigma - \omega_U^2(dL_U^2 - dR_U^2), \quad (3.20)$$

$$\Delta S = 2F_S(dR_S + dL_S)\sigma + \omega_S^2(dL_S^2 - dR_S^2), \quad (3.21)$$

$$U_k = [\dot{Q}^U(t_k)]^2, \quad S_k = [\dot{Q}^S(t_k)]^2. \quad (3.22)$$

From the energy equation for  $Q^{U,S}$  [derived from Eqs. (3.2)] and Eqs. (3.17) and (3.18),

$$U_1 = \omega_U^2(dR_U)^2 + 2F_U dR_U, \quad (3.23)$$

$$U_{k+1} = U_k + \Delta U, \quad S_{k+1} = S_k + \Delta S, \quad (3.24)$$

$$U_k = BS_k, \quad S_k = BU_k. \quad (3.25)$$

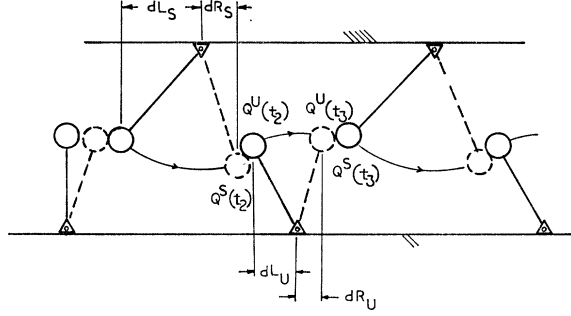


Fig. 5. Progress of the dislocation in terms of the pendulum analogy of local coordinate motion.

From the above, recurrence relations may be derived whose solution is<sup>11</sup>

$$S_{2n+1} = S_1 + B^3 C(1 - B^{2n}) / (1 - B^2), \quad n \geq 0, \quad (3.26)$$

$$U_{2n+2} = U_2 + B^4 C(1 - B^{2n}) / (1 - B^2), \quad n \geq 0, \quad (3.27)$$

$$S_\infty = B(\Delta U + B\Delta S) / (1 - B^2), \quad (3.28)$$

$$U_\infty = B(\Delta S + B\Delta U) / (1 - B^2), \quad (3.29)$$

where

$$C = (1 - B^{-2})U_1 + B^{-1}\Delta S + B^{-2}\Delta U.$$

The time of traverse of a stable (unstable) pendulum acted on by a constant force  $F_{S,U}$  with initial displacement  $-dL_{S,U}$ , initial velocity  $S_k(U_k)$ , and final displacement  $dR_{S,U}$  is

$$\omega_S(t_{k+1}^S - t_k^S) \\ = \arcsin \left\{ \frac{dR_S - F_S \omega_S^{-2}}{[S_k \omega_S^{-2} + (dL_S + F_S \omega_S^{-2})^2]^{1/2}} \right\} \\ + \arctan[\omega_S S_k^{-1/2}(dL_S + F_S \omega_S^{-2})], \quad k \text{ even}, \quad (3.30)$$

$$\omega_U(t_{k+1}^U - t_k^U) \\ = \operatorname{arcsinh} \left\{ \frac{F_U \omega_U^{-2} + dR_U}{[U_k \omega_U^{-2} - (F_U \omega_U^{-2} - dL_U)^2]^{1/2}} \right\} \\ - \operatorname{arctanh}[\omega_U U_k^{-1/2}(F_U \omega_U^{-2} - dL_U)], \quad k \text{ odd}. \quad (3.31)$$

Since one stable-unstable cycle represents a dislocation displacement of one atomic spacing the transient and steady-state dislocation velocity,  $v_k$  and  $v$ , are

$$v_k = (t_k^S - t_{k-1}^S + t_{k+1}^U - t_k^U)^{-1}, \quad k \text{ even}, \quad (3.32)$$

$$v = (t_\infty^S - t_{\infty-1}^S + t_{\infty+1}^U - t_\infty^U)^{-1}. \quad (3.33)$$

#### Dynamic Peierls Stress

The dislocation fails to surmount its potential barrier if the argument of the  $\operatorname{arctanh}$  in Eq. (3.31) is less than unity.  $U_k$  approaches its steady-state value monotonically, so the minimum stress required to maintain steady-state dislocation motion, referred to

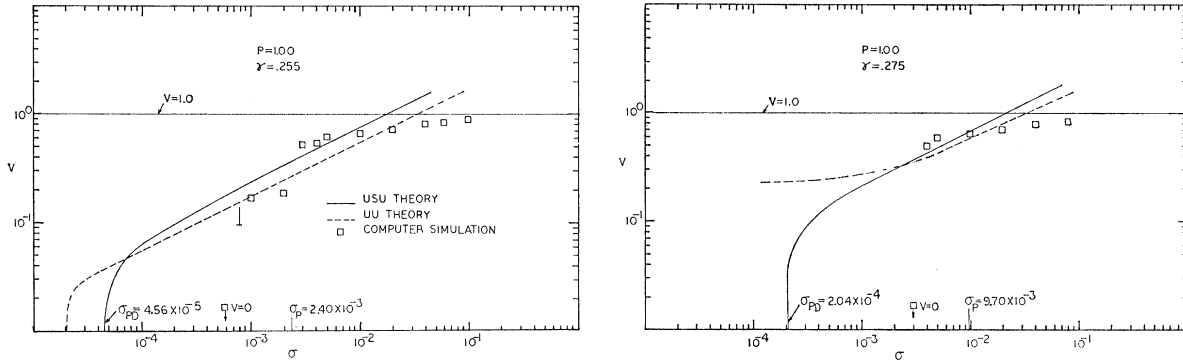


FIG. 6. Steady-state dimensionless dislocation velocity  $v$  as a function of applied dimensionless stress  $\sigma$ ; comparison of the  $UU$  and  $USU$  localized-mode theories with computer simulation for a finite lattice.

in Ref. 11 as the dynamic Peierls stress  $\sigma_{PD}$ , is found by solving  $\omega_U(F_U \omega_U^{-2} - dL_U)(U_\infty)^{-1/2} = 1$  for  $\sigma$ . Numerical values of  $\sigma_{PD}$  are shown in Fig. 6.

#### UU Motion

The unstable traverse which started when the weak bonds became  $1, j_w - 1$  and  $1, j_w$  ends when the weak bonds become  $1, j_w$  and  $1, j_w + 1$ . The short stable traverse is neglected. Then  $t_k$   $k$  odd ends an unstable traverse and  $t_k$   $k$  even begins an unstable traverse.  $Q^U(t_k)$   $k$  even ( $dL_U$ ) is given by Eq. (3.10), but  $Q^U(t_{k+1})$  is now given by (see Fig. 4)

$$Q^U(t_{k+1}) = v_{1,-1}^U / a_{1,-1}^U = (\frac{1}{2} + \gamma + U_{1,\frac{3}{4}}^a - 2U_{1,\frac{1}{4}}^a - \sigma) / a_{10}^U \equiv dR_U, \quad k \text{ even.} \quad (3.34)$$

At transition from one unstable traverse to the next

$$\dot{Q}^U(t_k) = B^{1/2} \dot{Q}^U(t_{k-1}), \quad k \text{ even,} \quad (3.35)$$

where now

$$B^{1/2} \equiv a_{ij}^U a_{i,j-1}^U < 1. \quad (3.36)$$

$UU$  motion may be interpreted by the pendulum analogy of the  $USU$  case, but with  $dL_S \equiv dR_S \equiv 0$  (see Fig. 5). With  $\omega_U^2$ ,  $U_k$ ,  $U_1$ , and  $\Delta U$  defined in Eqs. (3.19), (3.22), (3.23), and (3.20), the energy equation for  $Q^U$ , and Eq. (3.35), become

$$U_{k+1} = U_k + \Delta U, \quad k \text{ even,} \quad (3.37)$$

$$U_{k+1} = B U_k, \quad k \text{ odd.} \quad (3.38)$$

These lead to the steady-state condition

$$U_\infty = B(1-B)^{-1} \Delta U. \quad (3.39)$$

The time of traverse of the unstable pendulum is given by Eq. (3.31). Corresponding transient and steady-state velocities are

$$v_k = (t_{k+1}^U - t_k^U)^{-1}, \quad k \text{ even,} \quad (3.40)$$

$$v_\infty = (t_{\infty+1}^U - t_\infty^U)^{-1}. \quad (3.41)$$

Transient and steady-state velocities found from these equations are shown in Figs. 6 and 7.

#### IV. COMPUTER SIMULATION

As a check on the assumptions of this analysis, numerical computations on the IBM 7094 computer were made using the equations of motion with the time derivative in finite-difference form. The dislocation is started from unstable rest in the center of a finite lattice whose initial position is comprised of the zero-stress displacements  $u_{ij}^a$  and a uniform shear  $i\sigma$ . Uniform shear satisfies the equilibrium equations of all atoms except the weakly bonded ones and so they start to move first. The displacements  $u_{ij}^a$  are found for the finite lattice by an iteration procedure known as successive overrelaxation.<sup>22</sup> Both fixed and free boundaries are easily incorporated into the numerical procedure.

#### V. RESULTS AND DISCUSSION

##### Transient Velocities

The computer program for dislocation velocities was run for  $P=1.00$  and  $\gamma=0.255, 0.275$ ; a time increment of  $\Delta\tau=0.07$ , and a range of applied stress. For  $\gamma=0.255$  the stable traverse is very small and the  $UU$  theory should apply. For  $\gamma=0.275$  stable and unstable traverses are approximately equal and the  $USU$  theory should apply. Comparisons of computer simulation and  $UU$  theory are given in Figs. 7(a)–7(f) which show the velocity of the dislocation as a function of the number of atomic spaces it has moved through the lattice.

It was assumed that the dislocation had moved one atomic spacing when the atom on the slip plane representing its edge had moved one atomic spacing, i.e., had gone through a complete stable-unstable traverse. The time for moving one atomic spacing was measured from the instant a stable traverse began to the instant the succeeding stable traverse began. Then the velocity in dimensionless terms at that particular dislocation position is simply the reciprocal of the time in question. A velocity of 1 represents the velocity in

<sup>22</sup> R. S. Varga, *Matrix Iterative Analysis* (Prentice-Hall, Inc., Englewood Cliffs, New Jersey, 1962), p. 56.

the slip direction of plane dilational waves of infinite wavelength (velocity of sound in the continuum). The dislocation starts from unstable rest at the center of a lattice which has been given a uniform shear deformation  $i\sigma$ . All lattices in Fig. 7 are 20 rows by 120 columns except the one noted.

Fairly good agreement is shown up to a stress  $\sigma=0.02$ . Figure 7(a) typifies the increasing discrepancy between theory and computer simulation at higher stresses and velocities. There is qualitative agreement in the very rapid acceleration to a near steady-state velocity. At the lower stresses the effect of the finite size of the lattice becomes suspect. There is an attraction to the free boundary. This is clearly shown in Figs. 7(e) and 7(f). After the dislocation has moved 30 atomic spacings (halfway to the free boundary) and reached a steady-state velocity, there is a sharp increase in velocity. Increasing the width of the lattice to  $20 \times 180$  showed [Fig. 7(e)] that this was indeed a boundary effect. For a stress of  $\sigma=0.005$  it is difficult to discern a steady-state velocity. An increase in lattice width for this stress, however, gave results identical to those shown. One can conclude that at this and higher stresses, and for the distance travelled, increasing the lattice width had little effect on the dislocation velocity. For  $\sigma=0.004$  and  $\sigma=0.003$ , not shown, a  $20 \times 180$  lattice was used with results similar to Fig. 7(d). A test of the height effect was made by increasing the lattice size to  $30 \times 120$  for  $\gamma=0.275$  and  $\sigma=0.005$ . This choice of parameters was arbitrary, a systematic investigation of the height effect being impossible because of the large computer times involved. It was found that the dislocation moved somewhat slower, then somewhat faster, and then after about 10 atomic spacings the same as in a  $20 \times 120$  lattice. Halving the time increment to  $\Delta\tau=0.035$  for the case shown in Fig. 7(d) gave identical results, so that no significant error due to the finite-difference approximation to the acceleration is present in the results. The double-precision capability (16-place accuracy) of the IBM-7094 computer was used in these dynamic computations.

### Steady-State Velocities

From results such as shown in Fig. 7, steady-state velocities as a function of applied stress  $\sigma$  were found and are compared with both the  $UU$  and  $USU$  theory in Fig. 6. The  $UU$  theory is plotted for  $\gamma=0.275$  although the assumption of a small stable traverse does not apply. It is seen to agree quite well with the  $USU$  theory over a considerable range of applied stress  $\sigma$ . Both theories agree fairly well with the computer simulation for median velocities up to about 0.7 the speed of sound waves in the direction of slip.

Dislocation motion takes place below the Peierls stress but not at such low stresses as the theory predicts. This is probably due to the large amount of energy radiated from the dislocation at the very low velocities

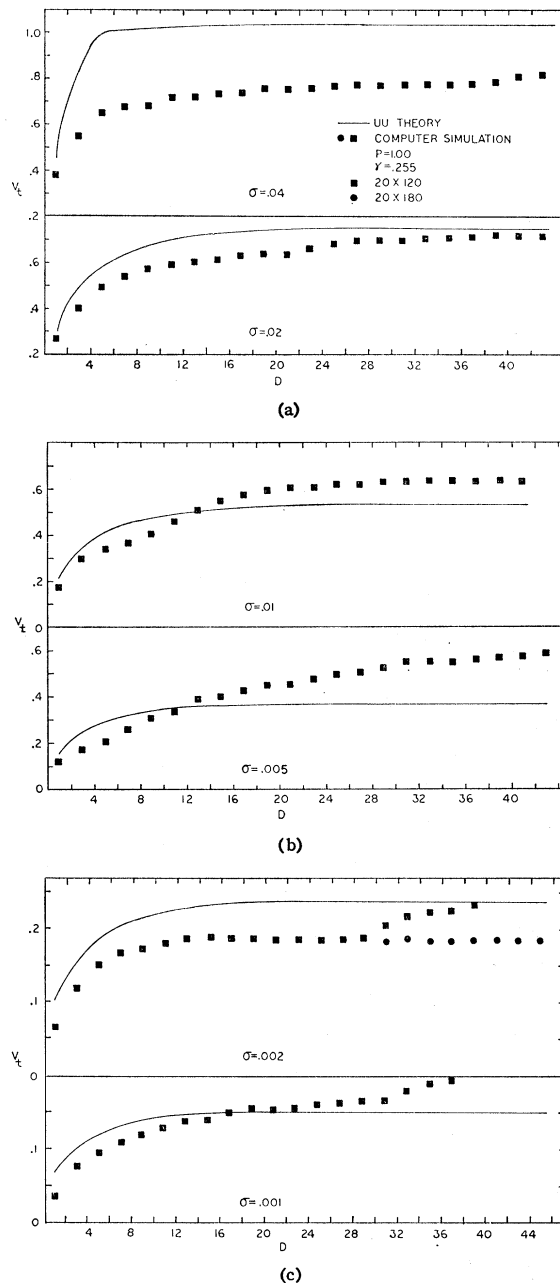


FIG. 7. Dimensionless dislocation velocity  $v_t$  as a function of distance  $D$  in atomic spacings. The  $UU$  (localized-mode) theory and the computer simulation for a finite free-boundary lattice are compared for various applied dimensionless stress  $\sigma$ . The dislocation starts at rest from the center of the lattice. A velocity of 1 corresponds to the velocity of plane dilational (sound) waves in the continuum in the slip direction.

which the dislocation has when starting from rest at these stresses. Not enough of the acquired kinetic energy remains in the neighborhood of the dislocation to enable it to overcome its next potential barrier. The discussion of Atkinson and Cabrera<sup>10</sup> on low-velocity dislocation motion appears relevant here.

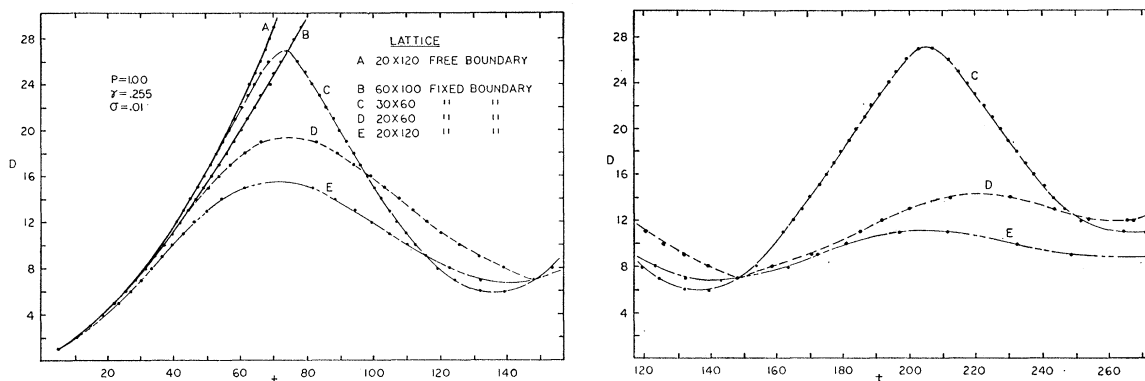


FIG. 8. Distance  $D$  in atomic spacings as a function of dimensionless time  $t$ , for fixed-boundary (except as noted) lattices of various size, as found by computer simulation. The dislocation starts at rest from the center of the lattice.

At velocities approaching the speed of sound the 1-2-1-2 weak bond sequence is disrupted and weak bonds spread out from various points along the slip plane. Dislocation velocity for this situation is meaningless. It occurs at  $\sigma=0.2$ .

There is remarkably little difference in the velocity-stress relation, for both theory and computer simulation, between the two values of  $\gamma$ . For the lower value of Peierls stress, dislocation motion can take place at lower values of stress, as one would expect. These facts seem to indicate that a change in Peierls stress changes only the lowest value of stress at which motion can take place, but not the velocity distribution above this stress.

The velocity-stress distribution given by Weiner<sup>11</sup> for the linear chain is similar to that shown in Fig. 6 for the two-dimensional model. An exact comparison, however, is difficult because the parameters which fix dislocation widths, stable and unstable regions, and normal-mode characteristics, are different because of the difference in dimensionality.

#### Effect of Fixed Boundaries

Finally, as a matter of interest, some results of fixing the boundary of the lattice are presented in Fig. 8 for various-size lattices at a value of  $\gamma=0.255$  and a stress of  $\sigma=0.01$ . The position of the dislocation, starting at rest from the center of the lattice, is given as a function of dimensionless time. With the upper boundary fixed, the dislocation behaves as an elastic

string fixed at one end and with the other end constrained to move in a straight horizontal line under an applied force. The free end oscillates about the equilibrium position under the applied force. In the  $20 \times 60$  lattice the dislocation moved further than in the  $20 \times 120$  lattice, in spite of the fact that the end boundaries of the lattice repel instead of attract. This is because initially, since the unstressed lattice was first allowed to reach equilibrium before fixing the boundaries, the dislocation thought it was in a free-boundary lattice and therefore was attracted more to the closer boundary of the  $20 \times 60$  lattice, and hence acquired more kinetic energy. Actually, a quantitative description would have to take into account the effect of both left and right boundaries and the variation in attraction (repulsion) with respect to distance from these boundaries. The static effect of fixed and free boundaries on an edge dislocation in a discrete lattice has been found by Southworth.<sup>23</sup> Extending the height to 30 rows gives the expected increase in dislocation mobility. For comparison purposes, a  $20 \times 120$  lattice with free boundary, and a very large  $60 \times 100$  lattice with fixed boundary, are also shown.

#### ACKNOWLEDGMENT

The authors wish to gratefully thank Professor W. T. Sanders for his interest in the work and for many valuable discussions and suggestions.

<sup>23</sup> H. Southworth, Jr., *J. Phys. Chem. Solids* **26**, 1649 (1965).